

Multispectral terrestrial lidar: state of the art and challenges

S. Kaasalainen

Department of Navigation and Positioning, Finnish Geospatial Research Institute – FGI, Masala, Finland

ABSTRACT: The development of multispectral terrestrial laser scanning (TLS) is still at the very beginning, with only four instruments worldwide providing simultaneous three-dimensional (3D) point cloud and spectral measurement. Research on multi wavelength laser returns has been carried out by more groups, but there are still only about ten research instruments published and no commercial availability. This chapter summarizes the experiences from all these studies to provide an overview of the state-of-the art and future developments needed to bring the multispectral TLS technology into the next level. Although the current number of applications is sparse, they already show that multispectral lidar technology has potential to disrupt many fields of science and industry due to its robustness and the level of detail available.

1 INTRODUCTION

Multispectral laser scanning enables target identification and analysis by combining both spectral and spatial features. Multi-wavelength airborne laser scanners are already on the market, such as the Optech Titan 3-channel airborne laser scanner, and an increasing number of applications are being published (e.g., Wichmann *et al.*, 2015, Matikainen *et al.*, 2017, Axelsson *et al.*, 2018). Conversely, multispectral terrestrial laser scanners (TLS) only exist as prototypes built by few individual research groups. This chapter summarizes the current status of multispectral TLS and discusses the challenges and future prospects of this emerging technology.

Today, there are a few multispectral TLS and active imaging projects, ranging from two-dimensional (2D) active spectral imaging, sometimes with a separate range measurement (Wei *et al.*, 2012, Manninen *et al.*, 2014), to instruments producing full-scale three-dimensional (3D) point cloud data (Douglas *et al.*, 2012, Powers and Davis, 2012, Hakala *et al.*, 2012, Danson *et al.*, 2014). There are also pointwise systems, where only the intensity is measured for spectral analysis, and waveform lidars for vertical profiling (Rall and Knox, 2004, Du *et al.*, 2016). Alternatively, a point cloud is constructed by combining data from separate monochromatic laser scanners (Gong *et al.*, 2015, Hartzell *et al.*, 2016, Elsherif *et al.*, 2018). While all these provide

important input for analyzing the multispectral laser returns, the main focus of this chapter is in the simultaneous capture of spectra and target 3D geometry.

The most obvious advantage of multispectral lidar has already been shown in the pioneering studies (cf. Wichmann *et al.*, 2015): no time gaps or registration errors exist between different colors (or spectral channels) or between geometric (topography) and spectral features, which improves the results compared to the traditional approach of combining point clouds with hyperspectral imagery (e.g., Guo *et al.*, 2011). Also, the target identification capability of active hyperspectral imaging enables a wide variety of applications. But the prospect of mapping spectral properties in 3D over the target and in the same spatial resolution as conventional lidars have not yet been fully utilized or even understood. Many of the studies on multispectral laser scanning have so far focused on spectral performance without including the spatial interpretation of the point clouds. For example, Du *et al.* (2016) present leaf nitrogen retrieval with a 32 channel lidar, but the topographic aspect is not considered. A similar approach was presented in Li *et al.*, (2014), who also focused on leaf spectral indices rather than point clouds. However one-shot acquisition of point cloud and spectral data will crucially increase the level of detail and information content available from the measurements. There is also the prospect of getting non-destructive and large scale data on the properties that have so far been measurable with destructive means only (Hakala *et al.*, 2015), but this idea still needs comprehensive studies with improved instruments, as well as systematic laboratory reference to be established as a method.

Radiometric calibration of lidar intensity has been studied for more than a decade by now. A comprehensive review on radiometric calibration methods, along with the basic physical concepts is provided in Kashani *et al.* (2015). They classify the levels of intensity processing according to the accuracy and information quality of the calibrated laser returns, starting from the digital numbers (raw intensity) available directly from the detector (level 0). Level 1 comprises the range or incidence angle correction, while in level 2, scaling or normalization, such as histogram correction, is carried out. Full radiometric calibration (level 3) results in values comparable to target reflectance, and requires the use of reference targets with known reflectance. The level 3 process is also termed as absolute radiometric calibration (Briese *et al.*, 2012).

Kashani *et al.* (2015) also identified some important knowledge gaps, such as difficulty in comparison with intensities obtained with different lidar instruments or variation between different wavelengths. That, plus the fact that lidar intensity is still somewhat underutilized, especially for TLS (Li *et al.*, 2016, Schofield *et al.*, 2016) has been one of the drivers for the development of multiple wavelength laser scanners. Radiometric calibration has sometimes been seen as a preliminary step towards multispectral lidar (Matikainen *et al.*, 2017). Using multiple channels also

enables the use of spectral ratios, which may in some cases help overcome the problem that the laser backscatter intensity does not directly represent the hemispherical reflectance and hence the target physical properties. Simultaneous data acquisition at different wavelengths enables the comparison of spectral differences or trends, which can sometimes be done without absolute radiometric calibration using only the range-corrected or normalized return intensity (Kashani *et al.*, 2015, Li *et al.*, 2016). This kind of approach usually works when changes in target properties are observed within the same experiment or with the same instrument. However, even the relative measurements are prone to errors caused by inaccuracy in sampling or calibration of the laser beam at different wavelengths. It has also turned out that the radiometric calibration is instrument specific (Calders *et al.*, 2017). In any case, rigorous radiometric calibration is necessary to be able to interpret physically the reflectance measurements available from multispectral TLS. It is also critical for combining and comparing results from different experiments.

This chapter aims to provide a comprehensive overview on the status of multispectral TLS so far. It also discusses some important challenges related to multispectral laser scanning in particular, although many of these problems are familiar to monochromatic TLS as well. Even though the number of currently existing multispectral TLS instruments is sparse, those few available already indicate the vast potential of this new technology. The chapter is organized as follows: Section 2 reviews the state-of-the-art in multispectral TLS and identifies some difficulties commonly met in instrument development and data analysis. Applications are summarized in Section 3, while Section 4 highlights some future aspects related to the technology.

2 MULTISPECTRAL TERRESTRIAL LIDAR: STATE-OF-THE-ART AND CHALLENGES

Even though the idea of active hyperspectral sensing has been available for almost two decades (Johnson *et al.*, 1999), the first multi-wavelength terrestrial laser scanner instruments were presented by Douglas *et al.* (2012), Powers and Davis, 2012, Hakala *et al.*, (2012), and Gaulton *et al.*, (2013). Research efforts for multispectral TLS technologies are slowly increasing. Some applications have been previously summarized by Eitel *et al.*, (2016) and Hancock *et al.*, (2017). Much of the research has focused on vegetation (Wichmann *et al.*, 2015).

2.1 State-of-the-art

Dual- or multi-wavelength 3D TLS point clouds have been published so far by four projects: the Dual-Wavelength Echidna Lidar (DWEL) (Douglas *et al.*, 2012) and the Salford Advanced Laser Canopy Analyser (SALCA) (Danson *et al.*, 2014) are dual wavelength instruments. The

Finnish Geospatial Research Institute Hyperspectral Lidar (FGI HSL) (Hakala *et al.*, 2012), and the spectral LADAR by Powers and Davis (2012) have multiple channels. All these are full waveform digitizing scanning lidars. In addition to these four, there are multispectral lidar studies that have mainly focused on spectral or waveform analysis of the laser return. Table 1 lists all these research efforts, followed by a more detailed description on each project in this section.

Table. 1: Summary of multispectral lidar projects. The top four provide one-shot multispectral point clouds, whereas the others focus on spectral analysis of pointwise or two-dimensional depth images.

Project	Laser Source	Channels (nm)	Detector/Sampling	Application
DWEL (Douglas <i>et al.</i> , 2012)	Two coaxial lasers, 5.1 ns, 20 kHz	1064, 1548	InGaAs photodiodes, 2 GHz digitizer	Separating leaves vs. bark
SALCA (Danson <i>et al.</i> , 2014)	Two asynchronous lasers, 1-3 ns, 5 kHz	1063, 1545	Single digitizer 1GHz	VI's related to moisture
FGI HSL (Hakala <i>et al.</i> , 2012)	Supercontinuum, 1 ns, 5 kHz	8 channels: 450-1050	Spectrograph, APD array, 1 GHz digitizer	Target identification, VI's
Spectral LADAR (Powers & Davis, 2012)	Supercontinuum, 1.8-4.0 ns, 25 kHz	25 channels: 1080–1620	Spectrograph, InGaAs APD, 5 GHz digitizer	Material type classification
MSCL (Woodhouse <i>et al.</i> , 2011)	Tunable Nd:YAG, 4.75ns, 20Hz	531, 550, 690, 780	Silicon photodiode + oscilloscope, 5 GHz	VI's such as PRI, NDVI
GECO (Eitel <i>et al.</i> , 2014a)	Two laser diodes, 1 kHz	532, 658	Red/green filters, two photodiodes	Chlorophyll observation
HSL Beijing (Li <i>et al.</i> , 2014)	Supercontinuum, 1-2 ns, 20-40 kHz	4-32 channels: 409-914	APD arrays, 5 GHz digitizer	Leaf biochemical contents
TCSPC Lidar (Wallace <i>et al.</i> , 2014)	Supercontinuum, < 50 ps, 2 MHz	531, 570, 670, 780	4 single photon APDs + TCSCP modules	Conifer needle NDVI
MSL Wuhan (Gong <i>et al.</i> , 2015)	4 synchronous diode lasers, 800 Hz	556, 670, 700, 780	4 PMT's, oscilloscope, range finder	Object classification
HL System (Du <i>et al.</i> , 2016)	Supercontinuum, 1–2-ns, 20–40 k Hz	32 channels: 538 - 910	Grating spectrometer, APD array	Rice leaf nitrogen from SVM

Note: VI = Vegetation Index APD = Avalanche Photodiode, PRI = photochemical reflectance index, NDVI = normalized difference vegetation index, TCSPC = Time-Correlated Single-Photon Counting, PMT = Photo Multiplier Tube, SVM = support vector machine.

2.1.1 Multispectral TLS providing 3D topography and reflectance information

Dual-Wavelength Echidna Lidar (DWEL) is a portable two channel scanning lidar developed at the Boston University (Douglas *et al.*, 2012, Howe *et al.*, 2015). Two coaxial near-infrared (NIR, 1064 nm) and shortwave infrared (SWIR, 1548 nm) lasers (with beam diameter of 7 mm), which are ideal for leaf separation, and are synchronized with an external trigger (Douglas *et al.*, 2015). An additional green laser is applied to be able to see the scan path. The returning pulses are collected with a telescope. Full waveforms are captured with two indium gallium arsenide (InGaAs) photodiode detectors, for which the beams are separated with a beam splitter. The measurement range is about 70 meters. A radiometric calibration scheme, based on reference panels, has recently been outlined to relate the measured reflectance to target radiative and structural properties (Li *et al.*, 2016). In addition to improving the quantitative results on vegetation structure from spectral responses, the calibration scheme also enables the comparison and collaborative use of different instruments.

Salford Advanced Laser Canopy Analyser (SALCA) (Gaulton *et al.*, 2013, Danson *et al.*, 2014) uses two sequentially emitting lasers. Full waveforms at NIR (1063 nm) and SWIR wavelengths (1545 nm) are detected and digitized with a single detector. These wavelengths have proven ideal in, e.g., leaf-bark separation. Because of the asynchronous pulses there is a small (1%) offset in the footprints. Calibration is done by means of reference panels. The maximum range is 105 m, and the footprint sizes are 8.0 mm (1063 nm) and 9.2 mm (1545 nm) at 10 m. The capability of the SALCA lidar in leaf water content retrieval has been demonstrated with normalized difference (vegetation) indices observed for three different species (Gaulton *et al.*, 2013). Recently, a radiometric calibration scheme based on neural networks was presented for SALCA (Schofield *et al.*, 2016). As the radiometric response to range, reflectance, and laser temperature was found to be complex, a neural network solution proved a robust tool for reflectance calibration. An effect of internal temperature on intensity was detected, and since it was more pronounced in SWIR, this might pose another challenge to multispectral lidar measurement and analysis in general.

The FGI Hyperspectral lidar (HSL) (Hakala *et al.*, 2012) is a multi-wavelength full waveform laser scanner, with a supercontinuum laser light source producing 1 ns pulses at 420–2400 nm (the spot size being 5mm at 4 m for 543 nm). The optical system consists of a parabolic mirror, which collects the returned pulse energy into an optical fiber connected to a spectrograph. The spectral dispersion is detected with an avalanche photodiode (APD) array (with 450–1050 nm response range). Currently, 8 of 16 available APD spectral channels can be digitized, but the APD array can be moved with respect to the spectrograph to adjust the wavelengths to be de-

tected. In the 2012 breadboard prototype, the digitizer operated on 1 GHz sampling rate, but increasing the digitization rate is investigated as a part of an ongoing development work towards an operational field instrument and improved target characterization (Kaasalainen *et al.*, 2018b). The ongoing development and intensity calibration efforts also aim at increasing the detector sensitivity and extending the measurement range from currently achieved 5-50 meters. Here too, external reference panels are used in the calibration.

The spectral Laser Detection And Ranging (LADAR) laboratory demonstrator prototype developed in Maryland by Powers and Davis (2012) is also based on supercontinuum technology. In addition to the supercontinuum source, the system comprises transmitter and receiver mirrors and optics, a mechanically tuned spectrometer, APD array driving a transimpedance amplifier (TIA), and a 5 GSa/s digitizer. Similarly to the FGI HSL, the time-of-flight measurement is triggered by picking up a fraction of the outgoing beam with a beam splitter. The measured range has been tested up to 40 m. The instrument was designed with military imaging applications in mind, and therefore its capability of detecting obscured objects from behind a camouflage was demonstrated. The near-infrared wavelengths of operation also ensure eye safety.

2.1.2 Lidar projects focusing on spectral analysis

There are also lidar studies, where mainly the intensity or the spectrum of the returning laser pulse is analyzed from a fixed point on the target surface. An instrument closest to a one-shot multi-wavelength lidar was introduced by Gong *et al.*, (2015). Their approach was based on Wei *et al.*, (2012), where a four-wavelength synthesized beam was produced with four semiconductor laser diodes (555, 670, 700, and 780 nm). Spatial data were obtained using a simultaneous laser range finder for distance measurement, which means that the spectral and spatial information would not come from the same source. The technical solution was described to be equivalent to four monochromatic lidars, but the combination of a single-wavelength point cloud and a multispectral image could be used for classification similarly to multispectral TLS. The study focused on classification algorithms for target identification, e.g., separating green and dry leaves and inorganic materials.

The Edinburgh University Multispectral Canopy Lidar (MSCL) is based on tuneable laser operation in four wavelengths: 531, 550, 690, and 780 nm (Woodhouse *et al.*, 2011). No point clouds were presented, but tree vertical structure was analysed from digitized waveforms, together with intensity information for analysing bark, twigs, and leaves. The full waveform configuration allowed the acquisition of canopy profile and NDVI with respect to tree height. The NDVI profiles could be related to chlorophyll concentration (Morsdorf *et al.*, 2009). Four wave-

lengths were also recorded with a time-correlated single-photon counting (TCSPC) technique by Wallace *et al.* (2014), which would also allow the collection of 3D depth image data. Supercontinuum laser was used as a source, but the output was filtered. The single photon counting approach was based on an earlier design by Buller *et al.* (2005). The TCSPC lidar was also used to produce underwater 3D depth images at a single wavelength (Maccarone *et al.*, 2015).

Crop foliar nitrogen retrieval was carried out with the Green Economic Chlorophyll Observation (GECO) sensor consisting of two laser diodes (532 and 658 nm) (Eitel *et al.*, 2014a). Only the returning laser intensity was analyzed, and range data were not utilized. A horizontal path lidar for chlorophyll estimation in two wavelengths were also presented by Rall and Knox, (2004).

Supercontinuum laser has been tested for target spectral analysis by Du *et al.* (2016) and Sun *et al.* (2017), who measured rice leaf nitrogen at 32 channels ranging from 538 to 910 nm. In this experiment, the laser was pointed to the target at a fixed incidence angle. A grating spectrometer was used for creating the dispersion of the returned supercontinuum laser pulse. Nitrogen content was retrieved and classified using the spectral data only. A similar approach with full waveform digitizing capacity was developed by Li *et al.* (2014) for measuring leaf biochemical contents, e.g., nitrogen. Point clouds were not presented either, but range measurement was tested in a later study (Niu *et al.*, 2015). They also investigated the ranging accuracy, but presented no 3D point clouds either.

2.2 Challenges

As multispectral TLS instruments are not available commercially, and because of the novelty of the technologies, there are many challenges related to hardware design, e.g., beam alignment in multi-laser systems, range accuracy, detector sensitivity (especially signal to noise), etc. (cf. Danson *et al.*, 2014, Howe *et al.*, 2014). Many of these are related to the fact that the laser power is dispersed into multiple channels. Also, much of the analysis is based on comparison of intensity values or trends, which emphasizes the need for consistent spectral performance to be able to separate reliably the hits from different targets. This causes extra work with data preprocessing, calibration, and information extraction (cf. Danson *et al.*, 2018).

Laser stability is vital for spectral performance. Temperature was found to affect the intensity of SALCA returns (Danson *et al.*, 2018). For DWEL, the drifts in laser power are monitored with a reference panel sampling the outgoing pulses during each mirror rotation (Li *et al.*, 2016). In the case of supercontinuum laser used in the FGI HSL, fluctuations in laser stability are normalized by dividing each pulse with the trigger pulse, which is separated from each transmitted pulse with a beam sampler. Initial tests have indicated a reasonable spectral stability, but the stability

is being further assessed in the ongoing calibration study (Kaasalainen *et al.* 2018b). Powers and Davis (2012) also use the transmitted pulse to normalize the backscattered signal.

Another important issue is the considerable data volume, especially when the number of channels and scanning resolution are increased. This introduces more demands for data processing, storage, and transfer, especially if on-site pre-processing is needed for real-time operation. Therefore, even if the addition of channels would be technically straightforward, for example by just adding another digitizer component, dealing with the increased data volume would require considerable changes in the processing and calibration procedures. Optimizing the processing steps is one of the future aims and the solutions are likely to be application specific. The challenges of processing, storing, and analyzing vast amounts of data produced by full waveform lidar in general have been addressed in many studies (e.g., Pfeifer *et al.*, 2014).

It is already known from single wavelength TLS that full waveform echo digitizing will improve not only the range, but also target detection capacity (Ullrich and Pfennigbauer, 2011). A lot of effort has been put into sampling the laser waveforms. As a pre-processing step, sampling is usually implemented by the manufacturer in commercial scanners (cf. Calders *et al.* (2017) who discuss the pulse sampling for RIEGL VZ-400 terrestrial lidar), but as multispectral lidars are research instruments, the sampling has to be individually solved in each case. Narrow width pulses can be expected from low signal returns (Danson *et al.*, 2018). This may not cause a major problem in, e.g., vegetation mapping, where strong differences between NIR and visible are easily observed. But for targets, for which the spectral differences are small (or multiple hits must be detected), or those with great variation in intensity, the inaccuracy of weak signals may be an issue, especially when the digitizing rate is the same order as the pulse width (e.g., sampling 1 ns pulses at 1 GHz) (Kaasalainen *et al.*, 2018b). Pulse width is also crucial for range resolution, which can also be improved in the full waveform case with signal processing approaches (Powers and Davis, 2012).

There are other effects, such as ringing artifacts (Hakala *et al.* 2012, Li *et al.*, 2016, Danson *et al.* 2018), and telescopic and saturation, which occur especially when scanning from near to far ranges (Li *et al.* 2016). There is another calibration challenge coming from far range measurements, where the signal to noise ratio falls and hence decreases the accuracy. Specifications, such as scanning resolution vs. beam divergence also need to be optimized (Li *et al.*, 2018). Niu *et al.* (2015) discovered a synchronization inaccuracy between wavelengths for a supercontinuum laser, which may affect the range accuracy. While solutions can be found for all these problems, there is still a great need for comprehensive data collection to be able to utilize better the combined spectral and point cloud information accurately and robustly. This is particularly true

because so few multispectral TLS instruments are available, and most applications are still to be developed. New applications are likely to call for further hardware and software development.

3 APPLICATIONS

3.1 Vegetation

While the potential of TLS in measuring vegetation structure can be utilized with monochromatic scanners, the added value from simultaneous spectral data is considerable. Woodhouse *et al.* (2011) identified some potential vegetation applications for multispectral lidar, such as mapping species composition, identifying healthy versus stressed canopies, monitoring the plant photosynthetic capabilities, or diagnostic monitoring via pigment concentrations. Many of these have since been tested with newly developed instruments. Vegetation targets are usually challenging, since they represent complex, multi-target situations, where each laser pulse is likely to hit more than one surface.

3.1.1 Monitoring the photosynthetic activity and health

Vegetation photosynthetic capacity is an important research topic because it is directly related to the role of forests as carbon sinks, which is important in understanding the dynamics of climate change and the global carbon cycle (Gaulton *et al.*, 2013, Wallace *et al.*, 2014). Vegetation health, productivity and stress level are related to the leaf biophysical parameters, such as, the amount of chlorophyll in plants. Chlorophyll can be monitored by measuring the changes in the so-called vegetation spectral red-edge and estimating the chlorophyll levels with various vegetation indices using values near the red-edge domain (Rall and Knox, 2004). Therefore, there is a strong research interest towards retrieving vegetation spectral indices with multispectral TLS. These indices were previously studied by means of passive remote sensing (e.g., Kalacska *et al.*, 2015, Jay *et al.*, 2017). Nevalainen *et al.*, (2014) provide a summary of 27 published vegetation indices and tested them for pine chlorophyll retrieval with the FGI HSL. The modified simple ratio (MSR) and the modified chlorophyll absorption ratio index (MCARI), where reflectance values at 705 and 750 nm (i.e., those near the spectral red edge) were utilized, were found to be most sensitive for chlorophyll estimation. Similar indices were later monitored throughout the growing season with the FGI HSL to demonstrate a non-destructive time series of pine chlorophyll content, validated with laboratory analysis (Hakala *et al.*, 2015).

In addition to forests, crop monitoring has also been explored. Nitrogen concentration in oat samples were derived from the FGI HSL data by means of the chlorophyll absorption ratio index (CARI), for which laser returns at reflectance 700 nm, 670 nm, and 550 nm were selected (Nevalainen *et al.*, 2013). Support vector machine regression was tested for nitrogen concentration in rice crops by Du *et al.* (2016). Here the number of wavelengths played a crucial role.

Vegetation moisture content is an important indicator of tree health, drought stress, and fire risk. Moisture content has been mapped from SALCA point clouds using SALCA normalized ratio index (SNRI) and other indices, where laser return intensities at 1064 nm and 1545 nm were compared (Gaulton *et al.*, 2013, Hancock *et al.*, 2017). A relationship was found between equivalent water thickness (EWT) and SALCA reflectance at both channels, but the relationship was strongest with EWT and spectral indices. The suitability of SALCA wavelengths for leaf moisture estimation was also demonstrated with a leaf reflectance model.

3.1.2 *Identifying tree parts or tree species*

DWEL and SALCA have also been applied in the separation of leaf (foliage) and woody material (such as bark) to be able to study forest structure and function (Douglas *et al.*, 2015, Danson *et al.*, 2018). The recognition is based on the stronger leaf absorption at 1548 nm compared to stems, resulting in a difference between the intensities from two NIR channels, which can then be observed for each point. This improves substantially the separation capability, since for monochromatic laser scanners, even the waveform is not enough to separate hits from leaves with partial hits from edges of trunks or branches (Douglas *et al.*, 2015). Leaves can also be separated by point cloud classification using vegetation indices such as NDVI for each point (Woodhouse *et al.*, 2011, Nevalainen *et al.*, 2014).

Tree species classification has been demonstrated for spruce and pine with the FGI HSL (Vauhkonen *et al.*, 2013) based on classification features that combined range and reflectance properties. The returns from inside the foliage turned out to be essential with respect to the classification accuracy. The results are somewhat similar to those obtained with a multispectral airborne laser scanning at three wavelengths with Optech Titan X (Axelsson *et al.*, 2018), where combined spectral and range information proved most efficient in classification.

3.2 Object classification

3.2.1 Separating different materials

Multispectral TLS has also been used to separate inorganic materials from organic ones or each other (see Figure 1 for an example). Initial tests of the FGI HSL have been carried out to explore its potential for other applications than vegetation. Monitoring target moisture has been tested for cardboard and wooden objects in indoor conditions with spectral indices related to water absorption band at 970 nm (Kaasalainen *et al.*, 2017). Moisture in targets can be detected from these indices, while it can be automatically localized from point cloud information. Preliminary results for snow surfaces have also been obtained, mainly to explore the capability of the HSL to distinguish pollution or to investigate the possible wavelength effects on the incidence angle on snow (Anttila *et al.*, 2016). The incidence angle behavior was found to be similar for all HSL wavelengths (540-1000 nm) for a sample of melting (wet) snow. An ongoing research effort focuses on mineral identification in mines, where ores are distinguished from their spectral properties and mapped from 3D point clouds of mine tunnels. In comparison with strong signatures in the vegetation red edge domain, mineral detection has proven somewhat more challenging, as the differences in intensity are more subtle and hence pose more challenges to the accuracy of the radiometric calibration (Kaasalainen *et al.*, 2018b).

Gong *et al.*, (2015) used both spectral and spatial information to classify and distinguish different objects with the Wuhan MSL: white wall, ceramic pots, *Cactaceae*, carton, plastic foam block, and healthy and dead leaves, with a support vector machine (SVM) supervised classification method. The point clouds were obtained by combining a multispectral image captured with four lasers, and range information from a traditional lidar. Comparison of results to those from single wavelength lidar or traditional passive remote-sensing only indicated that a higher classification was achieved with simultaneous multispectral and spatial data.

3.2.2 Defense and security applications

There has been a long interest in active spectral imaging for military applications. Besides target classification, detection of concealed targets, e.g., those behind a camouflage nets have been an object of interest (Johnson *et al.*, 1999, Nischan *et al.*, 2003, Powers and Davis, 2012). Other important features in defense and security related imaging are the eye safety and the capability of long range measurement, even up to 1 km (Manninen *et al.*, 2014). 3D spectral point clouds have been utilized by Powers and Davis (2012), who demonstrated the advantages over passive spectral sensing in the detection of featureless, flat surfaces and objects obscured by camouflage

netting with a spectral LADAR operating in NIR. The separation was based on the range difference and spectral features, using a K-means algorithm for classifying spectral vectors.

Puttonen *et al.* (2015) applied the FGI HSL for identifying artificial targets (camouflage net, LECA brick, plastic chair) and separating them from vegetation. It was found that while the differences in spectral responses were significant and allowed classification, spatial aggregation of individually classified points increased the classification accuracy. This would mean that point cloud segmentation is necessary for a robust solution. It was also shown that spectral data enhance the detection of hidden targets (those masked with camouflage nets) using a combination of spectral indices (cf. Johnson *et al.*, (1999), who introduced this idea along with the concept of active hyperspectral imaging).

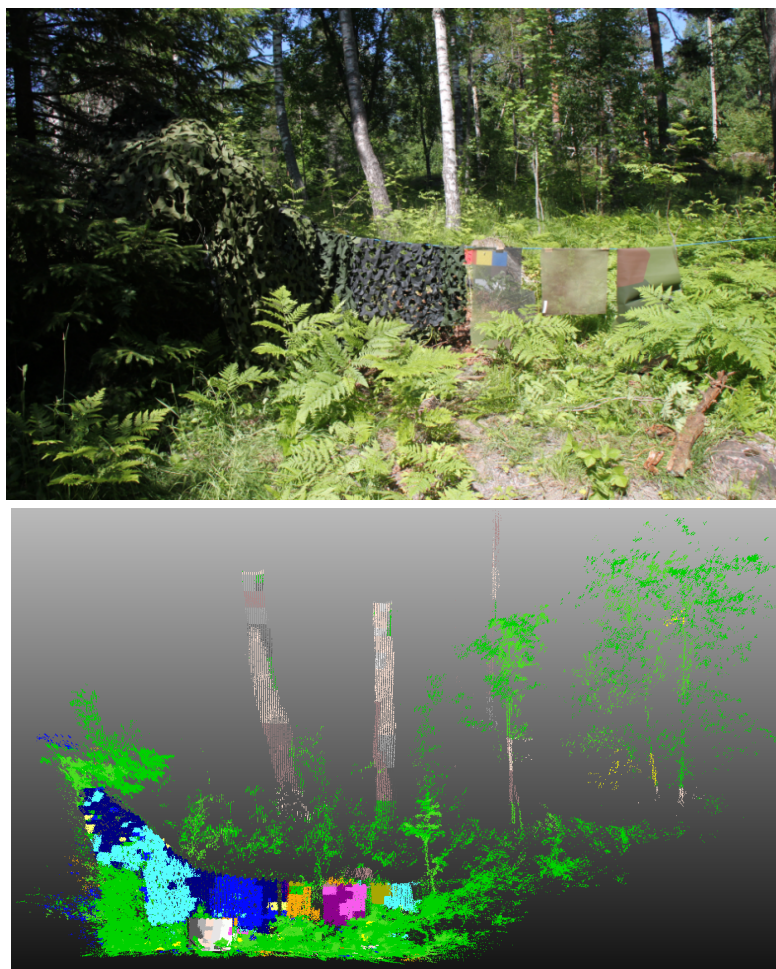


Figure 1: Example of target identification from a multispectral point cloud: camouflage and artificial targets can be separated from vegetation based on both spectral and shape recognition. The same applies for tree trunks and leaves. Point cloud obtained with the FGI HSL (Hakala *et al.*, 2012, Nevalainen *et al.*, 2014, Puttonen *et al.*, 2015). Image by Olli Nevalainen, FGI.

4 FUTURE ASPECTS

Many of the results presented in this chapter are preliminary and first of their kind, and call for extensive future research, both to establish the method and to show its full value in different scientific and commercial applications. However, they all point out the potential in robust and automatic target identification and monitoring. Considering the robotics and automation megatrends related to, e.g., intelligent transport, smart agriculture, or the internet of things (IoT), all these developments call for robust sensor-based environment perception.

There is an ongoing trend in TLS towards portability, rapid data capture, and also cost efficiency. While the data quality may not be as high as with a high-performance lidar, the practicality of cost-effective, lightweight TLS instruments is likely to increase their usage and thus allow larger areas to be investigated in the first place (Paynter *et al.*, 2016 and references therein). These devices have the potential to complement and extend the spatial range of observations acquired with high performance ones. There will be a pressure for lower cost in the multispectral TLS applications as well, but the technology should first be well established, and currently this is only possible with high performance research instruments.

Further research is still needed for full spatial interpretation of multi/hyperspectral TLS data, especially to establish a non-destructive means for, e.g., mapping vegetation pigment concentrations in 3D for diagnostics (Eitel *et al.*, 2014b, Hakala *et al.*, 2015, Sun *et al.*, 2017) or automatic localization of moisture in built environment (Kaasalainen *et al.*, 2017). In addition to the technical issues described above, a few significant future aspects are discussed in more detail.

4.1 Data analysis methods

Producing and analyzing multi-channel point clouds is a demanding task: not only the instrumentation is challenging, but software needs to be capable of handling vast amounts information produced by different types of digitization equipment. This information has to be processed and calibrated with methods customized for each instrument, and finally converted into a form readable for data analysis software (which will also have to be custom made as standard software for multispectral lidar are nonexistent), and formats suitable for other users. The LASer (LAS) format already allows the addition of extra attributes to each point in a point cloud (e.g., RIEGL, 2012). Because of vast information content, automatizing these processes still requires a major effort and optimization, especially if real-time mapping is aimed at (such as that in simultaneous localization and mapping (SLAM)). All the recent studies call for more work on the data analysis front (Douglas *et al.*, 2015, Danson *et al.*, 2018, Kaasalainen *et al.*, 2018b).

Even though manual delineation of objects could be possible using the spectrum of even a single point, combined use of both spatial and spectral information will be necessary for the solutions to be automatic and robust (cf. Li *et al.*, 2018). The need of information is application specific. Puttonen *et al.*, (2015) also found that, because of the complexity of the targets such as trees, an individual laser return can have almost any intensity, and hence it is difficult to identify a source of a single return. It was also shown that more than one spectral index was needed to separate some camouflage objects from organic ones. Kaasalainen *et al.*, (2018a) found that for vegetation, leaf angles affect the spectrum of some plants, and a physical correction of this inaccuracy is not realistic. This may introduce uncertainty in the vegetation indices.

While spectral (vegetation) indices have played a major role in multispectral lidar studies so far, other detection methods, such as spectral unmixing algorithms (Powers and Davis, 2012, Altmann *et al.*, 2015) can be applied. This calls for increasing the number of channels (from two or four), which is most practical by the use of supercontinuum lasers. Du *et al.* (2016) suggested that adding more channels improves the classification accuracy in the SVM regression.

4.2 Measurement geometry

Effects of measurement geometry, in this case, the incidence angle must be better understood. They have recently been shown to affect the spectral indices measured with laser scanners (Eitel *et al.*, 2014a, Hancock *et al.*, 2017). It is not possible to correct these for leaf canopies since the leaf incidence angle is mostly not known. Therefore, an empirical correction scheme may turn out the only alternative for vegetation (Kaasalainen *et al.*, 2018a) but in any case, the variation in incidence angles is likely to limit the accuracy of leaf spectral data (Hancock *et al.*, 2017). Further work is also needed to find out whether or not the incidence angle behavior would be different for relative (such as NDVI) or absolute vegetation indices (MCARI) (cf. Nevalainen *et al.*, 2014). Gaulton *et al.* (2013) and Shi *et al.* (2015) did not observe the incidence angle effect, but discussed the use of relative indices to cancel out or reduce it. Some targets do not exhibit any difference between wavelengths, such as a sample of wet snow (Anttila *et al.* 2016). It is clear that more testing and further experiments are needed.

4.3 Eye safety vs. number of channels

Near-infrared lasers have provided useful in moisture estimation (Gaulton *et al.*, 2013, Manninen *et al.*, 2014) and it is possible to build systems that meet the eye safety requirements. Overall, the eye safety problem is easier to tackle with instruments operating at discrete laser wavelengths, because they are easier to detect as all laser power is concentrated on narrow

wavelength bands. The downside is the inaccuracy in the co-alignment of the laser beams (Li *et al.*, 2018). Then again, supercontinuum lasers provide the only way to increase the number of channels or make a hyperspectral implementation. For visible wavelengths, filtering is one option, especially if the number of channels can be limited. For experiments carried out in laboratory or indoor environment (such as tunnels), this problem may be solved with traditional laser safety measures (limiting the access, safety goggles, etc.). Furthermore, the need for laser power in supercontinuum applications may decrease along with improving detectors as the technical readiness level increases from prototype level, or the power can be otherwise lowered in close range experiments. In any case, hyperspectral TLS utilizing supercontinuum lasers may never be a multi-purpose instrument, but should be tailored for the purpose to optimize the laser safety vs. wavelength range. Technical solutions enabling versatility will be crucial.

5 SUMMARY

Multispectral lidars represent the next generation of terrestrial laser scanning. This chapter has reviewed the current state-of-the art and discussed the prospects and challenges related to instrumentation, usage, and data interpretation from multispectral TLS. Once these challenges have been tackled, multispectral TLS will provide comprehensive environment perception and target identification in an entirely new level of robustness, detail, and accuracy. It has already been shown with the applications demonstrated so far that multispectral TLS has the potential of disrupting many fields of science and industry. As it seems that the technical implementation will strongly depend on the application, commercial availability may have to wait until the performance of the technology has been better established. This is an object of active ongoing research with more and more results coming up in the near future.

REFERENCES

- Altmann, Y., Wallace, A., & McLaughlin, S. (2015). Spectral Unmixing of Multispectral Lidar Signals. *IEEE Transactions on Signal Processing*, 63(20), 5525–5534. <https://doi.org/10.1109/TSP.2015.2457401>
- Anttila, K., Hakala, T., Kaasalainen, S., Kaartinen, H., Nevalainen, O., Krooks, A., ... Jaakkola, A. (2016). Calibrating laser scanner data from snow surfaces: Correction of intensity. *Cold Regions Science and Technology*, 121, 52–59. <https://doi.org/10.1016/j.coldregions.2015.10.005>
- Axelsson, A., Lindberg, E., & Olsson, H. (2018). Exploring Multispectral ALS Data for Tree Species Classification. *Remote Sensing*, 10(2), 183. <https://doi.org/10.3390/rs10020183>

- Briese, C., Pfennigbauer, M., Lehner, H., Ullrich, A., Wagner, W., & Pfeifer, N. (2012). Radiometric calibration of multi-wavelength airborne laser scanning data. *ISPRS Annals of Photogrammetry, Remote Sensing and Spatial Information Sciences*, 1-7, 335–340. <https://doi.org/10.5194/isprsannals-I-7-335-2012>
- Buller, G. S., Harkins, R. D., McCarthy, A., Hiskett, P. A., MacKinnon, G. R., Smith, G. R., ... Rarity, J. G. (2005). Multiple wavelength time-of-flight sensor based on time-correlated single-photon counting. *Review of Scientific Instruments*, 76(8), 83112. <https://doi.org/10.1063/1.2001672>
- Calders, K., Disney, M. I., Armston, J., Burt, A., Brede, B., Origo, N., ... Nightingale, J. (2017). Evaluation of the Range Accuracy and the Radiometric Calibration of Multiple Terrestrial Laser Scanning Instruments for Data Interoperability. *IEEE Transactions on Geoscience and Remote Sensing*, 55(5), 2716–2724. <https://doi.org/10.1109/tgrs.2017.2652721>
- Danson, F. M., Gaulton, R., Armitage, R. P., Disney, M., Gunawan, O., Lewis, P., ... Ramirez, A. F. (2014). Developing a dual-wavelength full-waveform terrestrial laser scanner to characterize forest canopy structure. *Agricultural and Forest Meteorology*, 198–199, 7–14. <https://doi.org/10.1016/j.agrformet.2014.07.007>
- Danson, F.M., Schofield, L.A., & Sasse, F. (2018). Spectral and spatial information from a novel dual-wavelength full waveform terrestrial laser scanner for forest ecology. *Interface Focus*, 8(2), 20170049, <http://dx.doi.org/10.1098/rsfs.2017.0049>
- Douglas, E. S., Strahler, A., Martel, J., Cook, T., Mendillo, C., Marshall, R., ... Lovell, J. (2012). DWEL: A Dual-Wavelength Echidna Lidar for ground-based forest scanning (pp. 4998–5001). IEEE International Geoscience and Remote Sensing Symposium (IGARSS '12). <https://doi.org/10.1109/igarss.2012.6352489>
- Douglas, E. S., Martel, J., Li, Z., Howe, G., Hewawasam, K., Marshall, R. A., ... Chakrabarti, S. (2015). Finding Leaves in the Forest: The Dual-Wavelength Echidna Lidar. *IEEE Geoscience and Remote Sensing Letters*, 12(4), 776–780. <https://doi.org/10.1109/lgrs.2014.2361812>
- Du, L., Gong, W., Shi, S., Yang, J., Sun, J., Zhu, B., & Song, S. (2016). Estimation of rice leaf nitrogen contents based on hyperspectral LIDAR. *International Journal of Applied Earth Observation and Geoinformation*, 44, 136–143. <https://doi.org/10.1016/j.jag.2015.08.008>
- Eitel, J. U. H., Magney, T. S., Vierling, L. A., & Dittmar, G. (2014a). Assessment of crop foliar nitrogen using a novel dual-wavelength laser system and implications for conducting laser-based plant physiology. *ISPRS Journal of Photogrammetry and Remote Sensing*, 97, 229–240. <https://doi.org/10.1016/j.isprsjprs.2014.09.009>
- Eitel, J. U. H., Magney, T. S., Vierling, L. A., Brown, T. T., & Huggins, D. R. (2014b). LiDAR based biomass and crop nitrogen estimates for rapid, non-destructive assessment of wheat nitrogen status. *Field Crops Research*, 159, 21–32. <https://doi.org/10.1016/j.fcr.2014.01.008>
- Eitel, J. U. H., Höfle, B., Vierling, L. A., Abellán, A., Asner, G. P., Deems, J. S., ... Vierling, K. T. (2016). Beyond 3-D: The new spectrum of lidar applications for earth and ecological sciences. *Remote Sensing of Environment*, 186, 372–392. <https://doi.org/10.1016/j.rse.2016.08.018>

- Elsherif, A., Gaulton, R., & Mills, J. (2018). Estimation of vegetation water content at leaf and canopy level using dual-wavelength commercial terrestrial laser scanners. *Interface Focus*, 8(2), 20170041. <https://doi.org/10.1098/rsfs.2017.0041>
- Gaulton, R., Danson, F. M., Ramirez, F. A., & Gunawan, O. (2013). The potential of dual-wavelength laser scanning for estimating vegetation moisture content. *Remote Sensing of Environment*, 132, 32–39. <https://doi.org/10.1016/j.rse.2013.01.001>
- Gong, W., Sun, J., Shi, S., Yang, J., Du, L., Zhu, B., & Song, S. (2015). Investigating the Potential of Using the Spatial and Spectral Information of Multispectral LiDAR for Object Classification. *Sensors*, 15(9), 21989–22002. <https://doi.org/10.3390/s150921989>
- Guo, L., Chehata, N., Mallet, C., & Boukir, S. (2011). Relevance of airborne lidar and multispectral image data for urban scene classification using Random Forests. *ISPRS Journal of Photogrammetry and Remote Sensing*, 66(1), 56–66. <https://doi.org/10.1016/j.isprsjprs.2010.08.007>
- Hakala, T., Suomalainen, J., Kaasalainen, S., & Chen, Y. (2012). Full waveform hyperspectral LiDAR for terrestrial laser scanning. *Optics Express*, 20(7), 7119. <https://doi.org/10.1364/OE.20.007119>
- Hakala, T., Nevalainen, O., Kaasalainen, S., & Mäkipää, R. (2015). Technical Note: Multispectral lidar time series of pine canopy chlorophyll content. *Biogeosciences*, 12(5), 1629–1634. <https://doi.org/10.5194/bg-12-1629-2015>
- Hancock, S., Gaulton, R., & Danson, F. M. (2017). Angular Reflectance of Leaves With a Dual-Wavelength Terrestrial Lidar and Its Implications for Leaf-Bark Separation and Leaf Moisture Estimation. *IEEE Transactions on Geoscience and Remote Sensing*, 55(6), 3084–3090. <https://doi.org/10.1109/TGRS.2017.2652140>
- Hartzell, P., Glennie, C., Biber, K., & Khan, S. (2014). Application of multispectral LiDAR to automated virtual outcrop geology. *ISPRS Journal of Photogrammetry and Remote Sensing*, 88, 147–155. <https://doi.org/10.1016/j.isprsjprs.2013.12.004>
- Howe, G. A., Hewawasam, K., Douglas, E. S., Martel, J., Li, Z., Strahler, A., ... Chakrabarti, S. (2015). Capabilities and performance of dual-wavelength Echidna[®] lidar. *Journal of Applied Remote Sensing*, 9(1), 95979. <https://doi.org/10.1117/1.JRS.9.095979>
- Jay, S., Maupas, F., Bendoula, R., & Gorretta, N. (2017). Retrieving LAI, chlorophyll and nitrogen contents in sugar beet crops from multi-angular optical remote sensing: Comparison of vegetation indices and PROSAIL inversion for field phenotyping. *Field Crops Research*, 210, 33–46. <https://doi.org/10.1016/j.fcr.2017.05.005>
- Johnson, B., Joseph, R., Nischan, M. L., Newbury, A. B., Kerekes, J. P., Barclay, H. T., ... Zayhowski, J. (1999). Compact active hyperspectral imaging system for the detection of concealed targets. In A. C. Dubey, J. F. Harvey, J. T. Broach, & R. E. Dugan (Eds.) (p. 144). <https://doi.org/10.1117/12.357002>
- Kaasalainen, S., Ruotsalainen, L., Kirkko-Jaakkola, M., Nevalainen, O., & Hakala, T. (2017). Towards multispectral, multi-sensor indoor positioning and target identification. *Electronics Letters*, 53(15), 1008–1011. <https://doi.org/10.1049/el.2017.1473>

- Kaasalainen, S., Åkerblom, M., Nevalainen, O., Hakala, T., & Kaasalainen, M. (2018a). Incidence Angle Dependency of Leaf Vegetation Indices from Hyperspectral Lidar Measurements. *Interface Focus*, 8(2), 20170033. <https://doi.org/10.1098/rsfs.2017.0033>
- Kaasalainen, S., Malkamäki, T., Ilinca, J., & Ruotsalainen, R. (2018b). Multispectral terrestrial laser scanning: new developments and applications. IEEE International Geoscience and Remote Sensing Symposium (IGARSS '18), accepted for publication.
- Kalacska, M., Lalonde, M., & Moore, T. R. (2015). Estimation of foliar chlorophyll and nitrogen content in an ombrotrophic bog from hyperspectral data: Scaling from leaf to image. *Remote Sensing of Environment*, 169, 270–279. <https://doi.org/10.1016/j.rse.2015.08.012>
- Kashani, A., Olsen, M., Parrish, C., & Wilson, N. (2015). A Review of LIDAR Radiometric Processing: From Ad Hoc Intensity Correction to Rigorous Radiometric Calibration. *Sensors*, 15(11), 28099–28128. <https://doi.org/10.3390/s151128099>
- Li, W., Sun, G., Niu, Z., Gao, S., & Qiao, H. (2014). Estimation of leaf biochemical content using a novel hyperspectral full-waveform LiDAR system. *Remote Sensing Letters*, 5(8), 693–702. <https://doi.org/10.1080/2150704X.2014.960608>
- Li, Z., Jupp, D., Strahler, A., Schaaf, C., Howe, G., Hewawasam, K., ... Schaefer, M. (2016). Radiometric Calibration of a Dual-Wavelength, Full-Waveform Terrestrial Lidar. *Sensors*, 16(3), 313. <https://doi.org/10.3390/s16030313>
- Li, Z., Schaefer, M., Strahler, A., Schaaf, C., & Jupp, D. (2018). On the utilization of novel spectral laser scanning for three-dimensional classification of vegetation elements. *Interface Focus*, 8(2), 20170039. <https://doi.org/10.1098/rsfs.2017.0039>
- Maccarone, A., McCarthy, A., Ren, X., Warburton, R. E., Wallace, A. M., Moffat, J., ... Buller, G. S. (2015). Underwater depth imaging using time-correlated single-photon counting. *Optics Express*, 23(26), 33911. <https://doi.org/10.1364/OE.23.033911>
- Manninen, A., Kääriäinen, T., Parviainen, T., Buchter, S., Heiliö, M., & Laurila, T. (2014). Long distance active hyperspectral sensing using high-power near-infrared supercontinuum light source. *Optics Express*, 22(6), 7172. <https://doi.org/10.1364/oe.22.007172>
- Matikainen, L., Karila, K., Hyypä, J., Litkey, P., Puttonen, E., & Ahokas, E. (2017). Object-based analysis of multispectral airborne laser scanner data for land cover classification and map updating. *ISPRS Journal of Photogrammetry and Remote Sensing*, 128, 298–313. <https://doi.org/10.1016/j.isprsjprs.2017.04.005>
- Morsdorf, F., Nichol, C., Malthus, T., & Woodhouse, I. H. (2009). Assessing forest structural and physiological information content of multi-spectral LiDAR waveforms by radiative transfer modelling. *Remote Sensing of Environment*, 113(10), 2152–2163. <https://doi.org/10.1016/j.rse.2009.05.019>
- Nevalainen, O., Hakala, T., Suomalainen, J., & Kaasalainen, S. (2013). Nitrogen concentration estimation with hyperspectral LiDAR. *ISPRS Annals of Photogrammetry, Remote Sensing and Spatial Information Sciences*, II-5/W2, 205–210. <https://doi.org/10.5194/isprannals-ii-5-w2-205-2013>
- Nevalainen, O., Hakala, T., Suomalainen, J., Mäkipää, R., Peltoniemi, M., Krooks, A., & Kaasalainen, S. (2014). Fast and nondestructive method for leaf level chlorophyll estimation using hyperspectral

- LiDAR. *Agricultural and Forest Meteorology*, 198–199, 250–258.
<https://doi.org/10.1016/j.agrformet.2014.08.018>
- Nischan, M., Joseph, R., Libby, J., and Kerekes, J. (2003) Active spectral imaging. *Lincoln Lab. Journal*, 14, 131–144. https://www.ll.mit.edu/publications/journal/pdf/vol14_no1/14_1activespectral.pdf
- Niu, Z., Xu, Z., Sun, G., Huang, W., Wang, L., Feng, M., Li, W., He, W., & Gao, S. (2015). Design of a New Multispectral Waveform LiDAR Instrument to Monitor Vegetation. *IEEE Geoscience and Remote Sensing Letters*, 12(7), 1506–1510. <https://doi.org/10.1109/LGRS.2015.2410788>
- Paynter, I., Saenz, E., Genest, D., Peri, F., Erb, A., Li, Z., ... Schaaf, C. (2016). Observing ecosystems with lightweight, rapid-scanning terrestrial lidar scanners. *Remote Sensing in Ecology and Conservation*, 2(4), 174–189. <https://doi.org/10.1002/rse2.26>
- Pfeifer, N., Mandlbürger, G., Otepka, J., & Karel, W. (2014). OPALS – A framework for Airborne Laser Scanning data analysis. *Computers, Environment and Urban Systems*, 45, 125–136.
<https://doi.org/10.1016/j.compenvurbsys.2013.11.002>
- Powers, M. A., & Davis, C. C. (2012). Spectral LADAR: active range-resolved three-dimensional imaging spectroscopy. *Applied Optics*, 51(10), 1468. <https://doi.org/10.1364/AO.51.001468>
- Puttonen, E., Hakala, T., Nevalainen, O., Kaasalainen, S., Krooks, A., Karjalainen, M., & Anttila, K. (2015). Artificial target detection with a hyperspectral LiDAR over 26-h measurement. *Optical Engineering*, 54(1), 13105. <https://doi.org/10.1117/1.oe.54.1.013105>
- Rall, J.A.R. & Knox, R.G. (2004). Spectral ratio biospheric Lidar. In IEEE International Geoscience and Remote Sensing Symposium, 2004 (IGARSS '04). Proceedings. 2004. IEEE.
<https://doi.org/10.1109/igarss.2004.1370726>
- RIEGL, 2012. LAS extrabytes implementation in RIEGL software, RIEGL Laser Measurement Systems GmbH.
http://www.cs.unc.edu/~isenburg/lastools/las14/Whitepaper_LAS_extrabytes_implementation_in_Riegl_software.pdf (Accessed Mar 15, 2018)
- Shi, S., Song, S., Gong, W., Du, L., Zhu, B., & Huang, X. (2015). Improving Backscatter Intensity Calibration for Multispectral LiDAR. *IEEE Geoscience and Remote Sensing Letters*, 12(7), 1421–1425. <https://doi.org/10.1109/lgrs.2015.2405573>
- Schofield, L. A., Danson, F. M., Entwistle, N. S., Gaulton, R., & Hancock, S. (2016). Radiometric calibration of a dual-wavelength terrestrial laser scanner using neural networks. *Remote Sensing Letters*, 7(4), 299–308. <https://doi.org/10.1080/2150704X.2015.1134843>
- Sun, J., Shi, S., Gong, W., Yang, J., Du, L., Song, S., ... Zhang, Z. (2017). Evaluation of hyperspectral LiDAR for monitoring rice leaf nitrogen by comparison with multispectral LiDAR and passive spectrometer. *Scientific Reports*, 7, 40362. <https://doi.org/10.1038/srep40362>
- Ullrich, A. & Pfennigbauer, M. (2011). Echo Digitization and Waveform Analysis in Airborne and Terrestrial Laser Scanning. In: Fritsch, D. (ed.) *Photogrammetric Week '11*. Wichmann/VDE Verlag, Belin & Offenbach, 2011. <http://www.ifp.uni-stuttgart.de/publications/phowo11/220Ullrich.pdf>
- Vauhkonen, J., Hakala, T., Suomalainen, J., Kaasalainen, S., Nevalainen, O., Vastaranta, M., ... Hyypä, J. (2013). Classification of Spruce and Pine Trees Using Active Hyperspectral LiDAR. *IEEE Geoscience and Remote Sensing Letters*, 10(5), 1138–1141. <https://doi.org/10.1109/lgrs.2012.2232278>

- Wallace, A. M., McCarthy, A., Nichol, C. J., Ximing Ren, Morak, S., Martinez-Ramirez, D., ... Buller, G. S. (2014). Design and Evaluation of Multispectral LiDAR for the Recovery of Arboreal Parameters. *IEEE Transactions on Geoscience and Remote Sensing*, 52(8), 4942–4954. <https://doi.org/10.1109/TGRS.2013.2285942>
- Wei, G., Shalei, S., Bo, Z., Shuo, S., Faquan, L., & Xuewu, C. (2012). Multi-wavelength canopy LiDAR for remote sensing of vegetation: Design and system performance. *ISPRS Journal of Photogrammetry and Remote Sensing*, 69, 1–9. <https://doi.org/10.1016/j.isprsjprs.2012.02.001>
- Wichmann, V., Bremer, M., Lindenberger, J., Rutzinger, M., Georges, C., & Petrini-Monteferrri, F. (2015). Evaluating the potential of multispectral airborne lidar for topographic mapping and land cover classification. *ISPRS Annals of Photogrammetry, Remote Sensing and Spatial Information Sciences*, II-3/W5, 113–119. <https://doi.org/10.5194/isprsannals-II-3-W5-113-2015>
- Woodhouse, I. H., Nichol, C., Sinclair, P., Jack, J., Morsdorf, F., Malthus, T. J., & Patenaude, G. (2011). A Multispectral Canopy LiDAR Demonstrator Project. *IEEE Geoscience and Remote Sensing Letters*, 8(5), 839–843. <https://doi.org/10.1109/LGRS.2011.2113312>